Applied Catalysis A: General 399 (2011) 42–49

Contents lists available at ScienceDirect

Applied Catalysis A: General

journal homepage: www.elsevier.com/locate/apcata

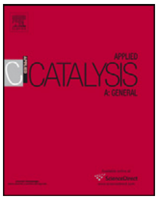

# Solvent free liquid-phase alkylation of phenol over solid sulfanilic acid catalyst

Farook Adam[a,*], Kasim Mohammed Hello[b], Tammar Hussein Ali[a]

[a] School of Chemical Sciences, Universiti Sains Malaysia, 11800 Penang, Malaysia
[b] Chemical Department, Collage of Science, Al-Muthanna University, Iraq

ARTICLE INFO

*Article history:*
Received 13 January 2011
Received in revised form 16 March 2011
Accepted 19 March 2011
Available online 26 March 2011

*Keywords:*
Surface modification
Sol–gel technique
Sulfanilic acid
Alkylation
4-*tert*-Butylphenol

ABSTRACT

Sulfanilic acid was immobilized onto rice husk ash via 3-(chloropropyl)triethoxy-silane to form an acidic solid catalyst denoted as $RHAPhSO_3H$. The BET surface area was found to be 308 $m^2\ g^{-1}$. Pyridine adsorption study revealed the presence of Brønsted acid sites. The EDX analysis showed the presence of S (10.88%) and N (10.37%). The $^{29}Si$ MAS NMR showed the presence of $T^2$, $T^3$, $Q^3$ and $Q^4$ silicon centres. The three carbon atoms of the propyl group were evident from the $^{13}C$ MAS NMR together with a series of chemical shifts consistent with the presence of the benzene ring. In the alkylation of phenol using $RHAPhSO_3H$ as the catalyst resulted in 95% conversion of *tert*-butyl alcohol at 120 °C with 52% selectivity towards 4-*tert*-butylphenol. The catalyst was reused several times without significant loss of catalytic activity.

## 1. Introduction

In recent years, the study of heterogenation of important organic ligands including important homogeneous catalysts onto suitable supports has seen increased interest due to the demand for green chemistry and environmentally friendly technologies. Rice husk (RH) is a by-product of the rice milling industry. These husks cause serious disposal and pollution problems due to the presence of a high content of silica. The controlled burning of RH in air leads to the formation of rice husk ash (RHA) which contains ca. 95% silica [1].

The main method of immobilization of the organic moieties was via the reaction of a particular molecule with the silanol groups on the silica surface. Typically such a process took about 12 to 24 h under reflux conditions [2–4]. In this respect, we had described the surface functionalization of silica with 3-(chloropropyl)triethoxysilane (CPTES) using a simple method which does not require toxic reagents [5]. The CPTES immobilized silica was used to heterogenize several organic molecules such as saccharine and melamine [6,7].

The alkylation of phenol is of great industrial importance. Some 450,000 tonnes of alkylated products like tertiary butylphenols are used in the industry per year. Mono-alkylphenols and di-alkylphenols are used in the manufacture of antioxidants, UV absorbers and for the production of phenolic resins [8,9]. Literature review reveals that these alkylation reactions are mostly carried out in the gas phase with high conversion of phenol [10,11]. However, gas phase reactions usually involve high temperature and pressure leading to high cost. Very few studies on the solvent state alkylation of phenol with tertiary butyl alcohol (TBA) have been published [12,13]. These solvent state reactions however, usually show very low conversions, i.e., less than 50%. It will therefore be advantageous to find new environmental friendly catalysts and milder experimental conditions to increase output to reduce cost and satisfy the environmental needs at the same time.

In this work, sulfanilic acid was immobilized onto silica from rice husk ash via CPTES to form an acidic solid catalyst. The catalyst was used successfully for the solvent free liquid-phase alkylation of phenol. Herein we report the preparation, characterization and the catalytic activity of this solid sulfanilic acid catalyst.

## 2. Experimental

### 2.1. Chemicals

The chemicals used in this study were sodium hydroxide (Systerm, 99%), CPTES (Sigma–Aldrich, 95%), sulfanilic acid (Sigma–Aldrich, 99%), nitric acid (Systerm, 65%), toluene (J.T. Baker, 99.8%), acetic acid (Systerm, 99.5%), TBA (Merck, 99%), phenol (Scharlau, 99.5%), acetonitrile (Qrec, 99.9%) and acetophenone (Nacalai tesque, 99.9%). The rice husk (RH) was collected from a rice mill in Penang, Malaysia. All chemicals were AR grade or of high purity and used directly without further purification.

---

* Corresponding author. Tel.: +60 1 64069717; fax: +60 4 6574854.
*E-mail addresses:* farook@usm.my, farook_dr@yahoo.com (F. Adam).

0926-860X/$ – see front matter © 2011 Elsevier B.V. All rights reserved.
doi:10.1016/j.apcata.2011.03.039

### *2.2. Extraction and modification of silica from RHA*

#### *2.2.1. Sources of silica*

The rice husk ash (RHA) was chosen as the source of amorphous silica [14] as it was available in abundance. The silica was extracted from rice husk according to a reported method [15,16].

#### *2.2.2. Synthesis of RHAPhSO$_3$H*

RHA silica was functionalized with CPTES according to the method reported elsewhere [5]. The resulting, RHACCl was used to immobilize sulfanilic acid onto the silica surface. A 1.0 g sample of RHACCl was dispersed in 30 mL dry toluene. To this suspension, about 1.5 g (8.6 mmol) of sulfanilic acid was added followed by 1.2 mL (8.6 mmol) of triethylamine acting as a proton scavenger. The mixture was refluxed for 48 h at 110 °C to produce a brown solid. The product was filtered off and washed with toluene, dichloromethane and finally with acidified ethanol. The sample was dried at 110 °C for 24 h and ground to powder. The product yield was 1.85 g and was labelled as RHAPhSO$_3$H.

### *2.3. Sample characterization*

The RHAPhSO$_3$H was characterized by Powder X-ray diffraction (Siemens diffractometer, D5000, Kristalloflex). The nitrogen adsorption porosimetry was carried out on an automatic physisorption porosimeter (Autosorb-1 CLP, Quantachrom, USA). The FT-IR spectra were recorded on a PerkinElmer spectrometer (System 2000). The $^{29}$Si and $^{13}$C MAS NMR was obtained using a Bruker (DSX-300) machine at the NMR research centre in IIS Bangalore. The scanning electron microscopy (SEM) (Leica Cambridge S360) and energy dispersive spectrometry (EDX) (Edax Falcon System) were used to study the surface morphology of the catalysts. The TEM micrographs were obtained using Philips CM12 equipment. Thermogravimetric analysis (TGA) was performed using a TGA SDTA851$^{e}$ instrument.

### *2.4. The surface acidity of RHAPhSO$_3$H*

The sample together with a beaker of pyridine was placed in a desiccator equipped with a valve connection to a membrane vacuum pump (AMB Greiffenberger Antriebstechnik, model MZ2C, CE 2002/06). The system was evacuated for 1 h at a rate of 1.7 m$^3$ h$^{-1}$. The system was then closed and the desiccator was kept under vacuum for 48 h to equilibrate. The atmosphere in the desiccator was evacuated again for 1 h at the same pumping rate. The sample was then removed and analyzed by FT-IR using KBr disc. The spectrum was recorded in absorption mode.

### *2.5. Cation exchange capacity (CEC)*

The cation exchange capacity (CEC) was done according to reported method [17]. Sodium chloride, 1.0 g was dissolved in 25 mL of distilled water in a conical flask with a magnetic stirrer. A 1.0 g (±10 mg) sample of RHAPhSO$_3$H was added and left to stir for 30 min. Phenolphthalein (2–3 drops) was added and the sample was titrated with standard NaOH solution. An average of 3 separate titrations were performed to obtain an average value for the cation exchange capacity of RHAPhSO$_3$H.

### *2.6. tert-Butylation of phenol*

The alkylation was carried out in liquid phase under argon in a 50 mL round bottom flask, equipped with a magnetic stirrer and water condenser. The water for the condenser was chilled to 2–3 °C in ice. A pump (Astro 500 liquid filter) was used to circulate this chilled water through the condenser to minimize the evaporation of TBA. Phenol (3.7 g, 0.04 mol) was transferred to the round bottom flask containing 0.15 g of the catalyst (pre-dried at 110 °C for 24 h and cooled in a desiccator to minimize moisture content). After the reaction temperature reached 120 °C, TBA (7.6 mL, 0.08 mol) was added. The reaction mixture was refluxed for 9 h. Samples for analysis (~0.50 mL) were withdrawn at regular intervals from the reaction mixture and 20 μL of acetonitrile (as internal standard for TBA) and or acetophenone (as internal standard for phenol) was added to the mixture. This mixture was then analyzed by GC and the products were confirmed by GC–MS.

## 3. Results and discussion

The synthesis of RHAPhSO$_3$H is shown in Scheme 1. The immobilization of sulfanilic acid onto RHACCl was done under reflux condition in dry toluene for 48 h. The following chemical and physical analyses were used to support the successful immobilization of sulfanilic acid.

### *3.1. The elemental analyses*

The elemental analysis showed the presence of 0.59% of N (10.37% by EDX). Sulphur was determined by EDX and showed 10.88% in RHAPhSO$_3$H. These elements were not present in RHACCl and RHA [5]. From the amount of Cl present in the EDX of RHACCl (4.08%) and RHAPhSO$_3$H (0.6%), the percentage loading of sulfanilic acid on the silica was calculated to be 87.5%. The results also show an increase in the percentage of C at 16.72% for RHAPhSO$_3$H compared to RHACCl.

### *3.2. Fourier transformed infrared spectroscopy analysis*

The FT-IR spectra of RHACCl and RHAPhSO$_3$H are shown in Fig. 1. The FT-IR spectra of RHA and RHACCl had been described previously by Adam et al. [5]. The typical broad band around 3458 cm$^{-1}$ is usually assigned to O–H vibration of SiO–H and HO–H of adsorbed water [18]. The stretching absorption band of NH appeared at 3198 cm$^{-1}$. The stretching vibration of C–H aromatic ring was observed at 3064 cm$^{-1}$. The stretching aliphatic C–H vibration was observed at 2929 cm$^{-1}$. The band at 1633 cm$^{-1}$ was assigned to the bending vibration of trapped water molecules within the silica matrix. The peaks at 1602–1547 cm$^{-1}$ could be due to the C=C bond. The asymmetric and symmetric stretching of the O=S=O fragment was observed at 1319, 1157 and 1114 cm$^{-1}$ respectively. The Si–C stretching vibration was observed at 1244 cm$^{-1}$. The band at 1075 cm$^{-1}$ was attributed to the Si–O–Si stretching vibrations in RHACCl. This peak had shifted to 1035 cm$^{-1}$ in RHAPhSO$_3$H. The FT-IR spectrum gives a good indication of the successful immobilization of the sulfanlic acid onto RHACCl.

### *3.3. Powder X-ray diffraction pattern*

The X-ray diffraction pattern (not shown) shows a broad peak at ca. 22.36°, which indicated the amorphous nature of the sample. This was similar to the observed diffraction pattern for amorphous silica in RHA and RHACCl as reported earlier [5].

### *3.4. N$_2$ adsorption–desorption analysis*

Fig. 2 shows the nitrogen adsorption isotherm obtained for RHAPhSO$_3$H with the inset showing the pore size distribution graph. The hysteresis loop observed in the range of $0.4 < P/P_0 < 1.0$, is associated with capillary condensation according to IUPAC classification. The isotherm exhibited by RHAPhSO$_3$H is of type IV and exhibited an H3 hysteresis loop [19].

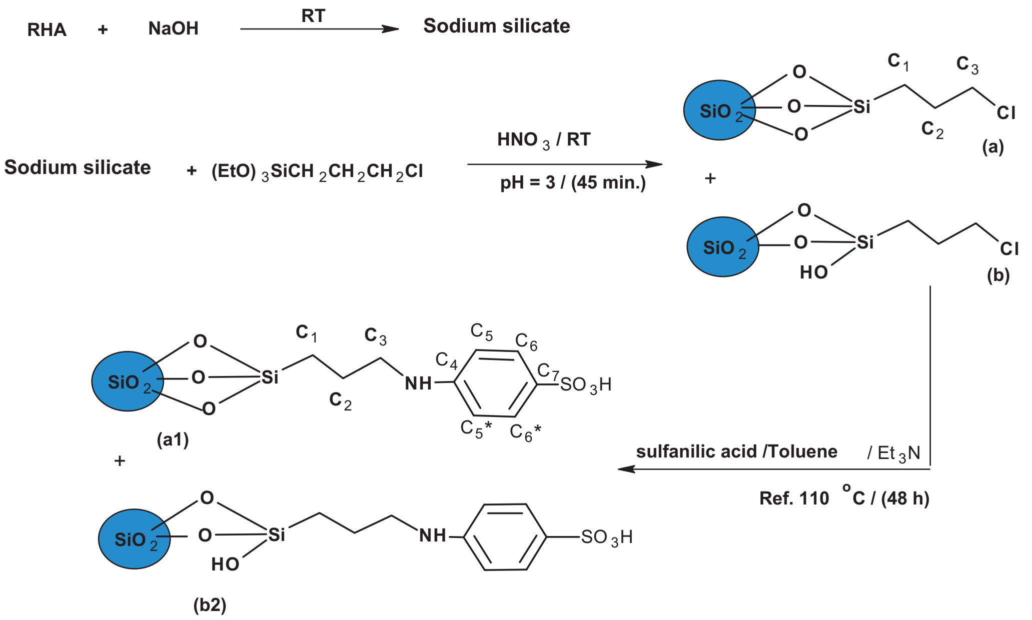

**Scheme 1.** The reaction sequence for the synthesis of RHAPhSO$_3$H. Two possible structures of the catalyst are postulated based on $^{13}$C and $^{29}$Si MAS NMR spectral studies. The approximate times taken for the completion of the experimental process are also shown.

The specific surface area of RHAPhSO$_3$H was found to be 308 m$^2$ g$^{-1}$ with an average pore volume of 0.6 cm$^3$ g$^{-1}$. The pore size distribution of RHAPhSO$_3$H reveals a narrow pore size range of ca. 4 - 7 nm. This can be advantageous as it can accommodate only specific size range of molecules in its pores, leading to catalytic selectivity. The specific surface area of RHACCl was 633 m$^2$ g$^{-1}$ with an average pore volume of 0.7 cm$^3$ g$^{-1}$ [5]. The decrease in the surface area of RHAPhSO$_3$H, however, could be due to the reduction of the surface sites due to the immobilization of sulfanilic acid causing the surface to be over crowded with the ligand network on the surface and thus blocking the smaller pores.

### 3.5. $^{29}$Si MAS NMR

The $^{29}$Si MAS NMR spectra of RHA [16] showed only the presence of Q$^4$ (Si(OSi)$_4$) and Q$^3$ (Si(OSi)$_3$(OH)) silicon centres', having chemical shifts at −110 and −100 ppm, respectively. The $^{29}$Si NMR spectrum of RHACCl showed chemical shifts attributed to Q$^4$ and Q$^3$ silicon atoms at −109.92 and −100.65 ppm respectively [5]. These chemical shifts were shifted to −110.9 and −100.9 ppm respectively in RHAPhSO$_3$H as shown in Fig. 3a. RHAPhSO$_3$H showed a chemical shift at −65.8 ppm which was assigned to the T$^3$ silicon centre. A similar chemical shift was observed at −65.2 ppm for RHACCl. The T$^2$ silicon centre in RHACCl was present at −57.4 ppm which was however shifted to −56.3 ppm in RHAPhSO$_3$H.

### 3.6. $^{13}$C MAS NMR

The $^{13}$C MAS NMR spectrum of RHAPhSO$_3$H is shown in Fig. 3b. It clearly shows three chemical shifts at 8.5, 24.7 and 45.5 ppm attributed to the C$_1$, C$_2$ and C$_3$ carbon atoms of the propyl chain (Scheme 1). Similar chemical shifts for RHACCl appeared at 10.3, 26.7 and 47.6 ppm, respectively [5].

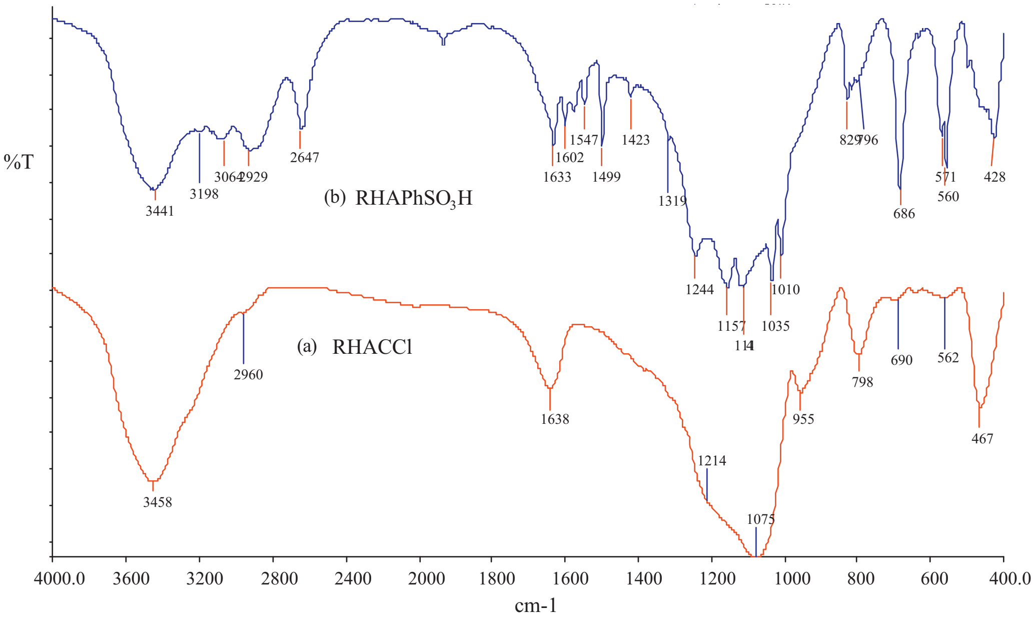

**Fig. 1.** The FT-IR spectra of (a) RHACCl and (b) RHAPhSO$_3$H.

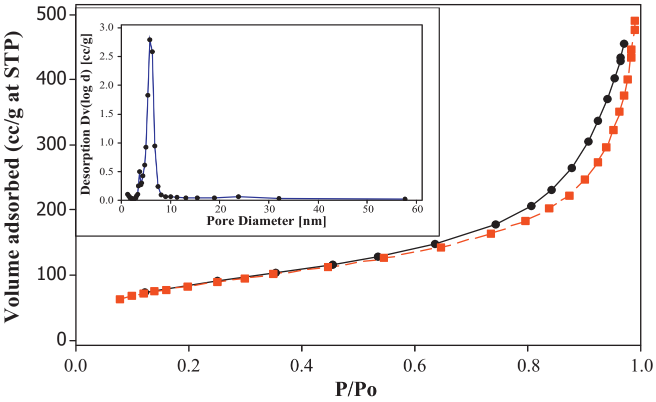

**Fig. 2.** The $N_2$ adsorption–desorption isotherm of $RHAPhSO_3H$. Inset shows the pore size distribution.

The broad chemical shifts at 120, 120.8, 121.2 and 124.8 ppm were assigned to the benzene ring (C4–C7). These results show that the sulfanilic acid was immobilized onto silica via the formation of the C–N bond as shown in Scheme 1.

### 3.7. Transmission electron microscopy

The scanning electron micrographs (SEM) are shown in Fig. 4a and b. The SEM shows that the sample is granular and porous. The granular particles of different sizes are arranged randomly on the surface building up the porous structure of the material.

Transmission electron micrographs (TEM) of $RHAPhSO_3H$ are also shown in Fig. 4c and d. The particles are irregular in shape and arranged in a non-orderly manner. These irregular particles may result from the non directional arrangement of pores due to the amorphous nature of the resulting material [20].

### 3.8. Thermal analysis by TGA FT-IR

The FT-IR spectrum (not showing) of the evolved gasses from TGA analysis (TGA-FTIR) was used to characterize each mass loss. The TGA of $RHAPhSO_3H$ showed four characteristic decomposition stages: the first starting at 34–142 °C, assigned to water loss (ca. 2.45%) which was confirmed by the FT-IR. The second mass loss (ca. 6.60%, 0.67 mg) occurred between 142 and 357 °C, assigned to the decomposition of sulfanilic acid on the silica surface. In accordance to this mass loss, it was calculated that 0.0039 mmol of sulfanilic acid was loaded on 10.25 mg of $RHAPhSO_3H$. Similar calculation had been reported for saccharine [6]. The third continuous mass loss (ca. 11.68%) occurred between 357 and 499 °C, which was attributed to the decomposition of unreacted chloropropyl group anchored on the silica. The fourth mass loss (ca. 10.60%) in the range 499–892 °C was attributed to the decomposition of the remaining organic groups. The FT-IR for this mass loss showed the presence of $-CO_2-$, $C_4H_6O_2$ and $H_2O$ moiety. The loss of water, specifically resulting from the condensation of silanol groups to form siloxane structure at the higher temperature.

### 3.9. The surface acidity

The concentrations of exchangeable proton on the $RHAPhSO_3H$ was determined in water by exchanging the ionisable proton with excess $Na^+$ (from NaCl) followed by titrating the $H^+$ liberated with standard NaOH solution. The cation exchange capacity (CEC) was found to be 23.0 mmol per 100 g $RHAPhSO_3H$.

The nature of the acid sites on the surface of $RHAPhSO_3H$ was also studied qualitatively by pyridine adsorption and desorption experiment monitored by FT-IR spectroscopy. The FT-IR spectra (Supplementary 1) of $RHAPhSO_3H$ after pyridine adsorption show strong bands at 1484 and 1434 $cm^{-1}$ which are due to the interaction between adsorbed pyridinium ion and the surface Brønsted acid site [21]. No Lewis acid sites were revealed on the catalyst surface by this study.

### 3.10. Alkylation study

*Tert*-butylation of phenol using TBA was carried out over $RHAPhSO_3H$ by varying the phenol:TBA ratio. The products obtained were 2-(*tert*-butyl)phenol (2-TBP), 4-TBP and 2,4-di(*tert*-butyl)phenol (2,4-DTBP). Scheme 2 shows the reaction and the products detected over $RHAPhSO_3H$. Small amounts of *tert*-butylphenol ether (TBPE) and isobutene (IBE) and its dimmers were also observed.

#### 3.10.1. The effect of time on TBA conversion

The conversion of TBA as a function of time is shown in Fig. 5. Table 1 shows the product distribution and selectivity at selected time intervals. After 1 h, the conversion of TBA was ca. 19%. The TBPE and IBE were the main products. During the second hour, the formation of 2-TBP and 4-TBP was observed. The formation of 2,4-DTBP was observed after 6 h. As the reaction time increased further, the conversion of TBA and the selectivity of 2-TBP, 2,4-DTBP and 4-TBP increased, while the product selectivity towards TBPE and IBE decreased. The decrease in the selectivity of TBPE and IBE could be due to further reaction of these products in the presence of $RHAPhSO_3H$. The conversion of TBA approached 95% at 9 h (Fig. 5). At this instant calculation showed a 57% conversion of phenol. No change in the conversion of TBA after 9 h was observed. The optimized reaction time was thus found to be 9 h.

The reaction catalysed by 3.2 mg (0.019 mmol) of sulfanilic acid (homogenous) also showed 82.8% conversion of TBA. The yield contained 48% of 2-TBP, 22% of 4-TBP, and 25% of TBPE in the same reaction time. We believe this is the first report of sulfanilic acid

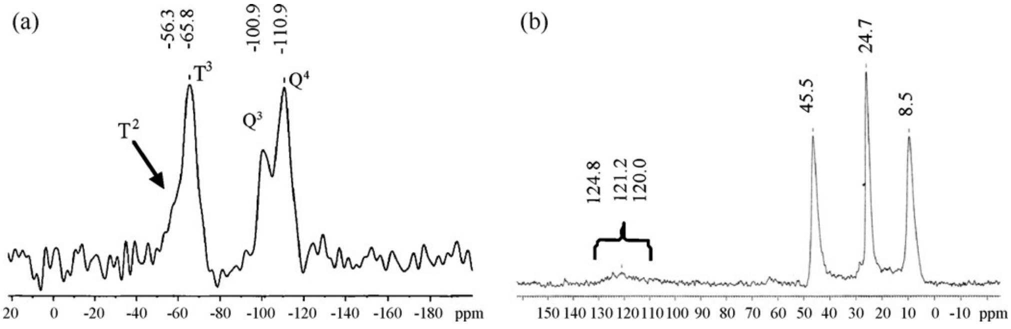

**Fig. 3.** The solid sate NMR spectra of $RHAPhSO_3H$. (a) The $^{29}Si$ MAS NMR spectrum (b) The $^{13}C$ MAS NMR spectrum.

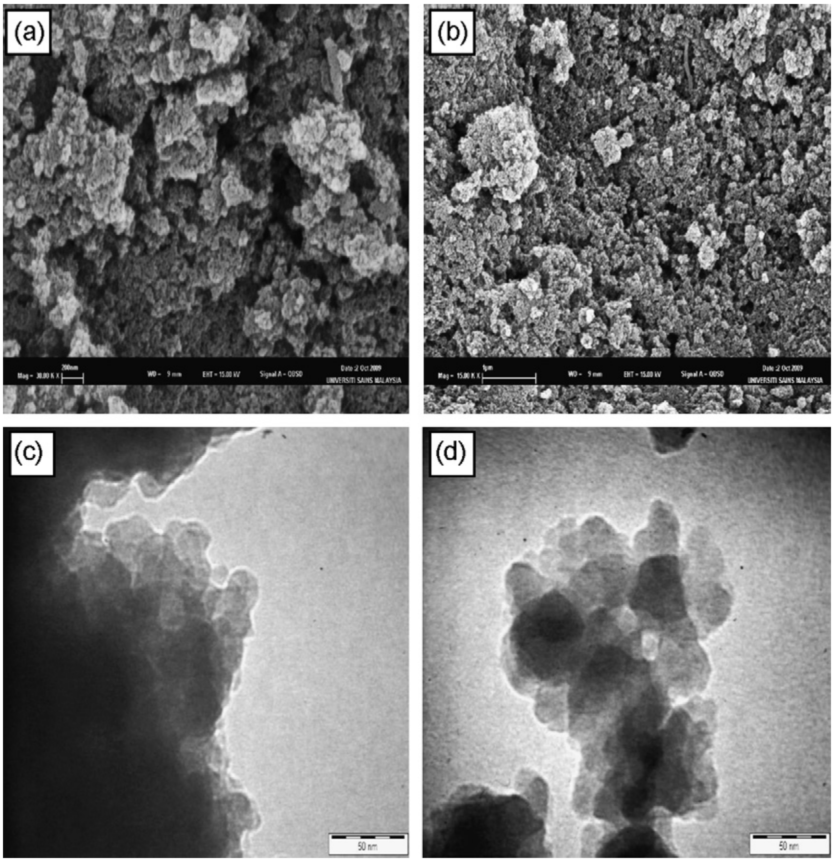

**Fig. 4.** The SEM and TEM images of RHAPhSO$_3$H: (a) SEM at 900k magnification, (b) SEM at 1500k magnification. (c and d) TEM at 260k magnification.

being used as a catalyst in a chemical reaction, be it homogeneous or heterogeneous. However, it is very clear that the heterogeneous RHAPhSO$_3$H is a much more efficient catalyst than the homogenous sulfanilic acid.

### *3.10.2. The effect of catalyst mass on the catalytic activity*

The influence of catalyst mass on the activity and selectivity of TBA was studied in the range of 25–200 mg of RHAPhSO$_3$H at 120 °C using 1:1 (phenol:TBA) mole ratio for 9 h. The product distribution and selectivity during each reaction time are shown in Table 2.

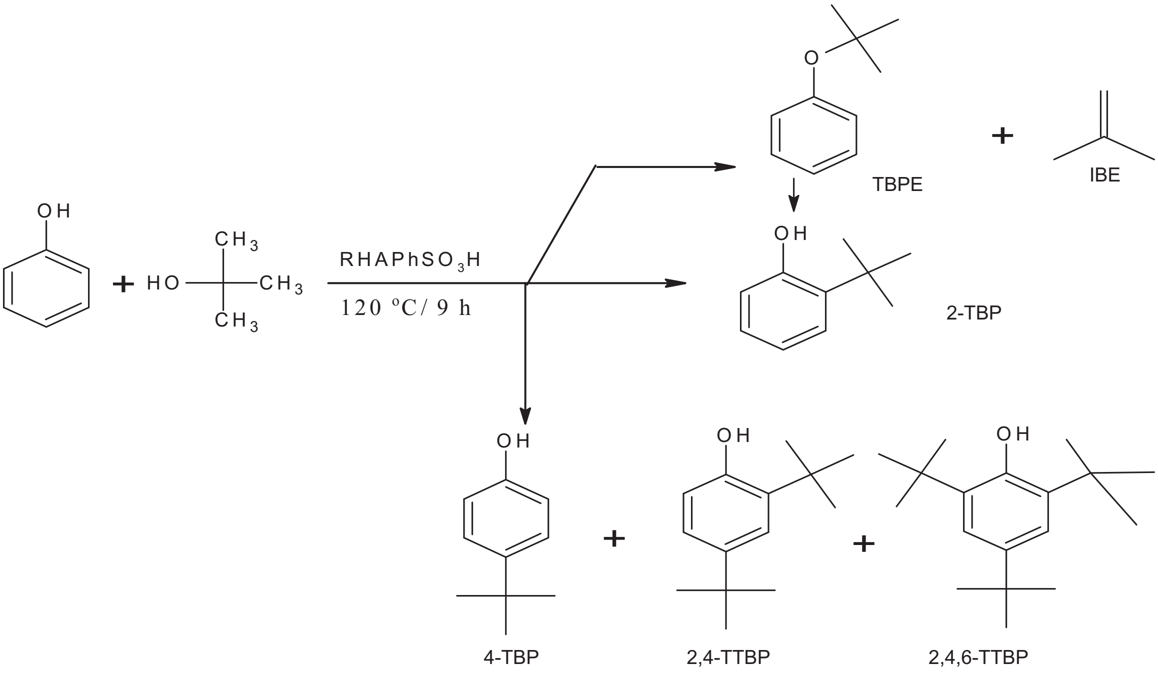

**Scheme 2.** *Tert*-butylation of phenol over RHAPhSO$_3$H and the structures of the products as determined by GC and confirm by GC–MS.

**Table 1**
Catalytic activity and product distribution as a function of reaction time. The reaction conditions: molar ration of phenol:TBA = 1:1, 50 mg mass of catalyst at 120 °C.

| Reaction time (h) | Conversion of TBA (mol%) | Selectivity of product (mol%) | | | | |
|---|---|---|---|---|---|---|
| | | 2-TBP | 4-TBP | 2,4-DTBP | TBPE | IBE |
| 0 | 0 | 0 | 0 | 0 | 0 | 0 |
| 1 | 10 | 2 | 0 | 0 | 87 | 10 |
| 2 | 26 | 3 | 1 | 0 | 89 | 7 |
| 3 | 32 | 4 | 2 | 0 | 90 | 4 |
| 4 | 44 | 8 | 3 | 0 | 82 | 7 |
| 5 | 66 | 16 | 7 | 0 | 70 | 7 |
| 6 | 82 | 26 | 10 | 1 | 56 | 7 |
| 7 | 86 | 40 | 17 | 4 | 32 | 6 |
| 8 | 90 | 49 | 21 | 4 | 23 | 3 |
| 9 | 95 | 52 | 23 | 5 | 16 | 3 |

**Table 2**
Catalytic activity and product distribution as a function of catalyst mass. The reaction conditions: molar ratio of phenol:TBA = 1:1, time 9 h, and temperature 120 °C.

| Catalyst amount (mg) | Conversion of TBA (mol%) | Selectivity of product (mol%) | | | | |
|---|---|---|---|---|---|---|
| | | 2-TBP | 4-TBP | 2,4-DTBP | TBPE | IBE |
| 25 | 85 | 44 | 19 | 3 | 27 | 6 |
| 50 | 96 | 53 | 23 | 5 | 17 | 3 |
| 100 | 95 | 52 | 23 | 5 | 16 | 3 |
| 200 | 81 | 43 | 18 | 3 | 30 | 5 |

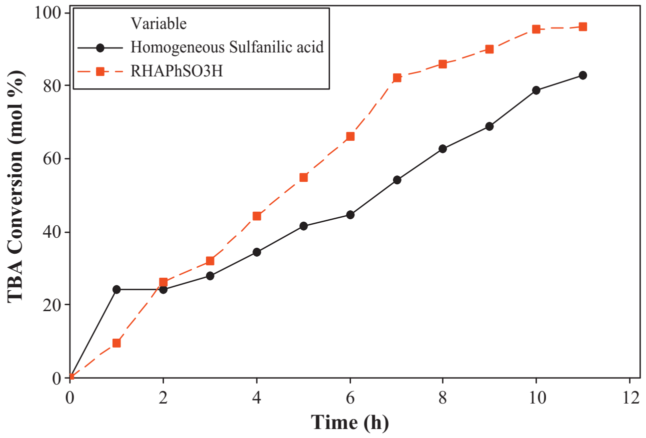

**Fig. 5.** Conversion of TBA in the alkylation of phenol with TBA over RHAPh$SO_3$H and homogeneous sulfanilic acid as a function of reaction time. Reaction conditions: molar ration of phenol:TBA = 1:1, mass of catalyst = 50 mg (3.2 mg homogenous catalyst) reaction temperature 120 °C.

When the catalyst mass was increased from 25 mg to 50 mg the conversion of TBA increased from 85 to 96% and the selectivity of 2-TBP reached ca. 53%.

When the catalyst mass was increased to 100 and 200 mg, the conversion of TBA decreased slightly. A two fold increase in TBPE was observed when the catalyst mass was 200 mg resulting in a decrease in the selectivity of 2-TBP (43%).

### *3.10.3. The effect of reaction temperature on the conversion of TBA*

The effect of temperature on the conversion of TBA and the catalytic performance was studied in the range of 100–120 °C and the results are summarized in Table 3. When the temperature increased the conversion and selectivity for all products increased. The selectivity for TBPE was observed to be very high (91%) at the lower temperature. This could be due to the molecular association that reduces adsorption and dissociation on the active sites [22]. This could also be due to the lower activation energy needed for etherification resulting in the formation of TBPE. Increasing the temperature to 120 °C results in a six fold decrease in TBPE and favours the formation of alkyl substitution on the ring. No product was observed at room temperature. However, in a control reaction where no catalyst was used, only TBPE was formed and the conversion of TBA was found to be ca. 8.63% after 9 h. This shows that the catalyst and the correct temperature are essential for the alkylation to take place.

### *3.10.4. The effect of reactant molar ratio*

The effect of the molar ratio of phenol:TBA on the conversion of TBA and the product selectivity is shown in Table 4. The result shows that the conversion of TBA increased progressively when the mole ratio was varied from 1:4 to 1:1. However, when the mole ratio was varied from 2:1 to 4:1, the TBA conversion decreased. The maximum conversion of 97% was obtained when the mole ratio of phenol:TBA was 2:1. However, the selectivity of 2-TBP was only 42% which was lower than the selectivity afforded by 1:1 mole ratio which was ca. 53% 2-TBP. Under the same condition the conversion of phenol was ca. 57%.

The conversion and selectivity for 2-TBP, 4-TBP and 4,2-DTBP decreased gradually when the mole ratio of TBA increased from 1:2 to 1:3. The selectivity of TBPE was 100% when the mole ratio was 1:4 at the percentage conversion of 15%. On the other hand, when the molar ratio was 4:1, the conversion of TBA was 81 mol%. This indicates that an over population of TBA will preferentially adsorb and block the active sites on the catalyst. This will reduce the possibility of reaction with the phenol. This is also a good indication that both reactants must be present side-by-side on the catalyst for reaction to take place. The catalytic reaction should thus be a second order $S_N2$ reaction, eliminating the possibility of free carbocation species leading to purely $S_N1$ reaction. Under the experimental condition, the kinetic data satisfies the pseudo-first order reaction kinetics in the presence of a large excess of one reactant. Given these experimental data, one could also essentially select etherification or alkylation products by simply selecting the appropriate mole ratio between phenol and TBA.

### *3.10.5. Reusability studies of RHAPhSO$_3$H*

The catalyst was regenerated by washing with ethanol and then dried at 170 °C for 24 h before each reuse. The elemental analysis (the value of EDX in bracket) for the regenerated catalyst showed

**Table 3**
The catalytic activity and the product distribution as a function of reaction temperature. The reaction conditions: molar ratio of phenol:TBA = 1:1, reaction time 9 h and mass of catalyst 50 mg.

| Temperature (°C) | Conversion of TBA (mol%) | Selectivity of product (mol%) | | | | |
|---|---|---|---|---|---|---|
| | | 2-TBP | 4-TBP | 2,4-DTBP | TBPE | IBE |
| 100 | 20 | 2 | 0.5 | 1 | 91 | 5 |
| 110 | 31 | 3 | 1 | 0.3 | 4 | 2 |
| 120 | 95 | 52 | 23 | 5 | 16 | 3 |

**Table 4**
The catalytic activity and the product distribution as a function of mole ratio. The reaction conditions: temperature 120 °C, time 9 h and 50 mg mass of catalyst.

| Molar ratio phenol:TBA | Conversion of TBA (mol%) | Selectivity of product (mol%) | | | | |
|---|---|---|---|---|---|---|
| | | 2-TBP | 4-TBP | 2,4-DTBP | TBPE | IBE |
| 1:4 | 15 | 0 | 0 | 0 | 100 | 0 |
| 1:3 | 27 | 1 | 3 | 1 | 93 | 2 |
| 1:2 | 50 | 6 | 2 | | 91 | 1 |
| 1:1 | 95 | 53 | 23 | 5 | 17 | 3 |
| 2:1 | 97 | 42 | 22 | 2 | 30 | 4 |
| 3:1 | 93 | 29 | 13 | 2 | 48 | 1 |
| 4:1 | 81 | 53 | 24 | 4 | 12 | 6 |

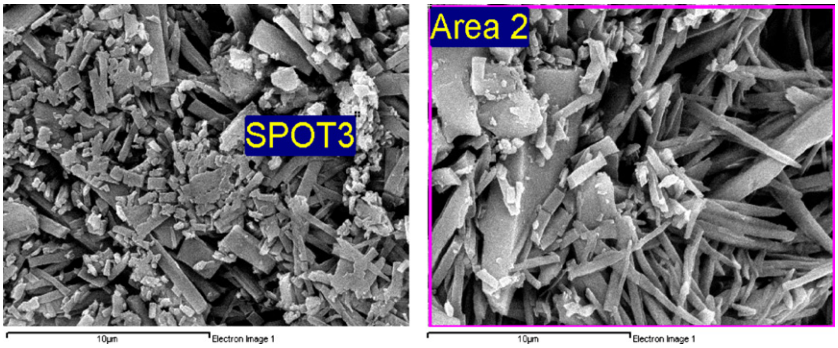

**Fig. 6.** The SEM images of used RHAPhSO$_3$H at 1.4k magnification.

the presence of N (10.17%), Cl (0.7%) and S (7.0%). The results did not show significant changes in these values. However, some change in the morphology of the surface was observed as in Fig. 6. The catalyst had agglomerated into rod shaped material. The result of the reusability study is shown in Table 5. The catalyst was found to be stable under the regeneration conditions and could be used several times without loss of catalytic efficiency.

### 3.10.6. *Reaction kinetics*

Kinetic parameters were obtained from experiments conducted at three different temperatures, i.e., 100, 110 and 120 °C. The reaction conditions for these experiments were 1:1 molar ratio of phenol:TBA, 50 mg catalyst mass and 9 h of reaction time. The data obtained from these experiments were used to determine the reaction kinetics of the catalyst (RHAPhSO$_3$H) as shown in Supplementary 2. It was observed that the experimental results obtained were in good agreement with the pseudo-first order rate law according to Eq. (1).

$$\ln\frac{1}{1-x} = k_a(t-t_0) \tag{1}$$

where $k_a$ is the apparent rate constant, $x$ is the fractional conversion of TBA, $t$ is the reaction time, and $t_0$ is the induction period.

The kinetic parameters for the catalyst are tabulated in Supplementary 3. The pseudo-first order rate constants were calculated from the slope of the experimental plots which gave the Arrhenius plot as shown in Supplementary 4. The apparent activation energy was deduced from the Arrhenius plot and was found to be 10.4 kcal mol$^{-1}$.

Krishnan et al. [8] evaluated the apparent activation energy ($E_a$) for the alkylation of phenol with *tert*-butyl alcohol under pressure in batch mode over various zeolite catalysts. The values obtained were greater than 6.5 kcal mol$^{-1}$. They concluded that the reaction was controlled by surface reaction. The value of $E_a$ obtained in this

**Table 5**
The conversion of TBA and the product selectivity in the alkylation of phenol as a function of reusability of catalyst. Reaction condition: molar ratio of phenol:TBA = 1:1, temperature = 120 °C, time 9 h and 50 mg catalyst.

| Catalyst | Conversion of TPA | Selectivity | | | | |
|---|---|---|---|---|---|---|
| | | 2-TBP | 4-TBP | 2,4-DTBP | TBPE | IBE |
| Fresh | 95 | 53 | 23 | 5 | 17 | 3 |
| 1 reuse | 96 | 50 | 24 | 11 | 4 | 4 |
| 2 reuse | 94 | 54 | 25 | 5 | 10 | 6 |
| 3 reuse | 94 | 51 | 22 | 3 | 17 | 6 |

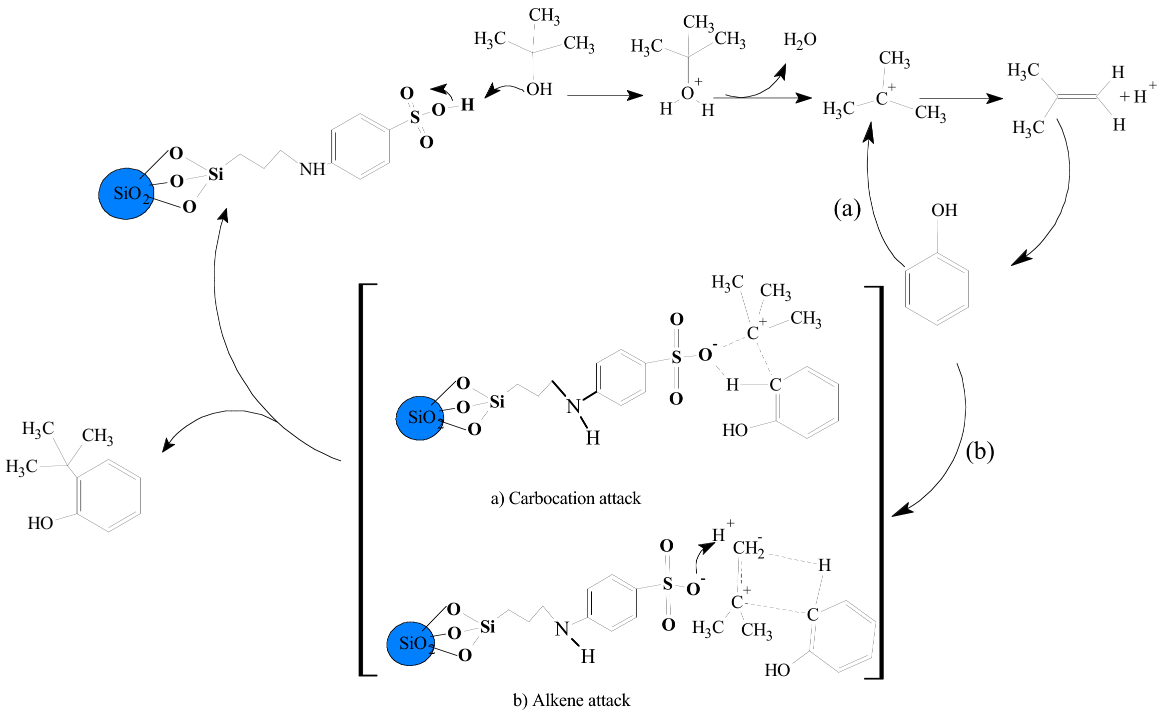

**Scheme 3.** The proposed mechanism for the *tert*-butylation of phenol over RHAPhSO$_3$H showing the formation of carbocation and the alkene intermediate. (a) The carbocation route and (b) the alkene route.

study is comparable in magnitude to that of the work of Krishnan et al. [8].

### 3.10.7. The proposed mechanism

The strong Brønsted acid sites in RHAPhSO$_3$H could protonate the hydroxyl group in TBA to form the oxonium ion which can easily liberate H$_2$O molecule to form the carbocation $(CH_3)_3C\oplus$ [23]. The formed carbocation could either directly attack the *ortho*- or *para*-position of phenol via formation of transition state (a) as shown in Scheme 3 to give the *ortho*- or *para*-alkyl phenol in a seemingly pseudo-first order reaction. The carbocation on the catalyst can also undergo elimination of proton to form the alkene which could also attack the *ortho* or *para* position of phenol via formation of transition state (b).

## 4. Conclusion

A simple and green technique was used to immobilize the sulfanilic acid to produce a solid Brønsted catalyst, RHAPhSO$_3$H. The RHAPhSO$_3$H showed promising catalytic activity for the liquid-phase *tert*-butylation of phenol using TBA. The catalyst was found to have a high selectivity to 2-*tert*-butylphenol and 4-*tert*-butylphenol. The catalysts could be reused several times without significant loss in their catalytic activity using mild regeneration technique.

## Acknowledgements

We would like to thank the Malaysian Government for the USM-RU-PRGS grant (1001/PKIMIA/842020) and RU grant (10001/PKIMIA/814019) which partly supported this work.

## Appendix A. Supplementary data

Supplementary data associated with this article can be found, in the online version, at doi:10.1016/j.apcata.2011.03.039.

## References

[1] F. Adam, M.Sc. Thesis, Universiti Sains Malaysia, (1991) p. 73.
[2] S.J. Bae, S.W. Kim, T. Hyeon, M. Kim, Chem. Commun. (2000) 31–32.
[3] X.Y. Shi, J.F. Wei, J. Mol. Catal. A: Chem. 280 (2008) 142–147.
[4] D. Hoegaerts, B.F. Sels, De.D.E. Vos, F. Verpoort, P.A. Jacobs, Catal. Today 60 (2000) 209–218.
[5] F. Adam, H. Osman, K.M. Hello, J. Colloid Interface Sci. 331 (2009) 143–147.
[6] F. Adam, K.M. Hello, H. Osman, Appl. Catal. A 365 (2009) 165–172.
[7] F. Adam, K.M. Hello, H. Osman, Appl. Catal. A 382 (2010) 115–121.
[8] A.V. Krishnan, K. Ojha, N.C. Pradhan, Org. Process Res. Dev. 6 (2002) 132–137.
[9] E. Modrogan, M.H. Valkenberg, W.F. Hoelderich, J. Catal. 261 (2009) 177–187.
[10] K. Song, J. Guan, S. Wu, Y. Yang, B. Liu, Q. Kan, Catal. Lett. 126 (2008) 333–340.
[11] S.E. Dapurkar, P. Selvam, Appl. Catal. A 254 (2003) 239–249.
[12] E. Dumitriu, D. Meloni, R. Monaci, V. Solinas, C. R. Chimie 8 (2005) 441–456.
[13] K. Ojha, N.C. Pradhan, A.N. Samanta, Chem. Eng. J. 112 (2005) 109–115.
[14] C. Real, M.D. Alcala, J.M. Criado, J. Am. Chem. Soc. 79 (1996) 2012–2016.
[15] F. Adam, J.H. Chua, J. Colloid Interface Sci. 280 (2004), 55–16.
[16] A.E. Ahmed, F. Adam, Micropor. Mesopor. Mater. 103 (2007) 284–295.
[17] F. Adam, L.F. Cheah, J. Por. Mater. 16 (2009) 291–298.
[18] F. Adam, S. Balakhrisnan, L.P. Wong, J. Phys. Sci. 17 (2006) 1–13.
[19] M. Thommes, Chem. Ing. Tech. 82 (2010) 1059–1073.
[20] F. Adam, J. Andas, J. Colloid Interface Sci. 311 (2007) 135–143.
[21] V. Luca, L. Kevan, C.N. Rhodes, D.R. Brown, Clays Clay Miner. 27 (1992) 515–519.
[22] V. Ajayan, K. Mani, M. Masahiko, M. Velayudam, A. Katsuhiko, J. Mol. Catal. A: Chem. 230 (2005) 151–157.
[23] K.U. Nandhini, J.H. Mabel, B. Arabindoo, M. Palanichamy, V. Murugesan, Micropor. Mesopor. Mater. 96 (2006) 21–28.